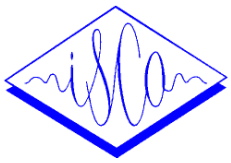

3rd International Conference on
Spoken Language Processing (ICSLP 94)
Yokohama, Japan
September 18-22, 1994

MEASUREMENT OF ACOUSTIC IMPEDANCE DENSITY DISTRIBUTION IN THE NEAR FIELD OF THE LABIAL HORN

Kunitoshi MOTOKI*, Pierre BADIN and Nobuhiro MIKI*****

* Faculty of Engineering, Hokkai-Gakuen University
S-26,W-11, Chuo-ku, Sapporo 064, JAPAN *motoki@eli.hokkai-s-u.ac.jp*

** Institut de la Communication Parlée-URA CNRS No368-INPG-Université Stendhal
46, Avenue Félix-Viallet, 38031 Grenoble Cedex 01, FRANCE *badin@icp.grenet.fr*

*** Faculty of Engineering, Hokkaido University
N-13,W-8, Kita-ku, Sapporo 060, JAPAN *miki@hudk.hokudai.ac.jp*

ABSTRACT

In this paper, a method for measuring the acoustic impedance density from sound pressure distribution is presented. Experiments were performed for a plaster replica of the lips together with the oral cavity and for a quasi-elliptical uniform tube with a wedged-shaped end imitating the lip horn. The change of frequency characteristics of the acoustic impedance density along the center-line inside the lips indicates that the labial horn acts as an acoustic wave guide. The theoretical characteristics of the acoustic impedance density derived from an idealized elliptical piston model and a pulsating sphere model are also shown for the better determination of the boundary condition for FEM computation.

1. INTRODUCTION

Recently, precise sound pressure measurement and numerical computation of the acoustic field in the vocal tract have been extended to take two-dimensional or three-dimensional effects of vocal tract geometry into account. Our previous experiments [1,2] that have been performed by using plaster replicas of the oral cavities have shown the existence of resonances in the transverse direction of the oral cavity, and similar results have also been reported in the numerical computation using Finite Element Method (FEM) [3]. Although FEM is considered as a useful method for analyzing the acoustic field in the vocal tract, proper boundary conditions at the lips are difficult to determine. In many cases, an equivalent lumped radiation impedance at the lips or the characteristic impedance of air at a relatively distant position from the lips has been used as a simplified boundary condition [4,5]. However, there has not been much discussion about the validity of these boundary conditions. A direct method would consist in measuring and analyzing the acoustic impedance density, defined as the ratio of sound pressure to particle velocity, in the near field of the labial horn.

In this paper, a method for measuring the acoustic impedance density from sound pressure distribution (SPD) is presented. Pure tones are used as a driving signal, and spatial distributions of amplitude and phase of sound pressure of each tone in the vicinity of the lips are measured by means of a small probe-microphone moved with the help of a computer controlled mechanical stage. Precise positioning of the probe-microphone is important in this method. Based on the measured SPD, first, particle velocity is computed using Euler's momentum equation, and then the trajectories of the medium particles are traced, which become ellipses in general. Then the acoustic impedance density is computed in the direction of the major axis of the elliptical trajectory of the medium particles.

Experimental results are presented for two specimens. One specimen is a plaster replica duplicating the actual shape of the lips and oral cavity, and the other one is a quasi-elliptical uniform tube with a wedged-shaped end roughly imitating the lip horn. Two-dimensional SPD's were measured on both vertical and horizontal planes. The frequency characteristics of the acoustic impedance density on these planes are presented.

As a result, for both specimens, the impedance density distribution along the center-line inside the lips shows that the labial horn acts as an acoustic wave guide. However, in the lateral regions of the lip horn, the vibration pattern of particles is less one-dimensional, especially at high frequencies. A map of particle trajectory could help defining a surface where, in every point, the particles have a one-dimensional motion only. This surface could then be used as the boundary on the lip side. The theoretical characteristics of the acoustic impedance density derived from an idealized elliptical piston model and a pulsating sphere model are also shown for the better determination of the boundary condition for FEM computation.

2. METHOD

2.1 Acoustic Impedance Density Computation

Let an instantaneous sound pressure of angular frequency ω at position $\mathbf{r}$ be $p_i(\mathbf{r},t)$. Using complex time factor $\exp(j\omega t)$, $p_i(\mathbf{r},t)$ can be written as

$$p_i(\mathbf{r},t) = P(\mathbf{r})\mathrm{Re}(\exp(j(\omega t + \phi(\mathbf{r})))), \quad (1)$$

where $P(\mathbf{r})$ and $\phi(\mathbf{r})$ are spatial distributions of amplitude and phase of sound pressure, which are to be experimentally measured. Then complex sound pressure distribution $p(\mathbf{r})$ and complex particle velocity $\mathbf{v}(\mathbf{r})$ can be related by Euler's momentum equation as

$$\nabla p(\mathbf{r}) + j\omega\rho\mathbf{v}(\mathbf{r}) = \mathbf{0}, \quad (2)$$

where ρ is air density and $p(\mathbf{r}) = P(\mathbf{r})\exp(j\phi(\mathbf{r}))$. Then $\mathbf{v}(\mathbf{r})$ can be solved as follows.

$$\mathbf{v}(\mathbf{r}) = (j\nabla P(\mathbf{r}) - P(\mathbf{r})\nabla\phi(\mathbf{r}))\exp(j\phi(\mathbf{r}))/\omega\rho \quad (3)$$

The acoustic impedance density $Z_d(\mathbf{r})$ is defined as the ratio of $p(\mathbf{r})$ to the directional component of $\mathbf{v}(\mathbf{r})$. If we use an xyz rectangular coordinate system, $Z_d(\mathbf{r})$ in x-direction, for example, can be computed as follows.

$$Z_d(\mathbf{r}) = \frac{\omega\rho P(\mathbf{r})}{j\dfrac{\partial P(\mathbf{r})}{\partial x} - P(\mathbf{r})\dfrac{\partial\phi(\mathbf{r})}{\partial x}} \quad (4)$$

In a two- or three-dimensional acoustic field, the phase of each directional component of $\mathbf{v}(\mathbf{r})$ may take different value, which results in the trajectories of the medium particles being ellipses. In that case, the dominant direction of the medium vibration, which is the direction of the major axis of particle trajectory, is selected as the direction of $Z_d(\mathbf{r})$ computation. In our practical procedure, first x- and y- (*or* z-) directional components of $\mathbf{v}(\mathbf{r})$ are computed, then the direction of the major axis of the particle trajectory is determined, and finally $Z_d(\mathbf{r})$ in this direction is computed using both x- and y- (*or* z-) directional components of $\mathbf{v}(\mathbf{r})$. As seen from eq.(4), the sensitivity of the probe-microphone, the gain of the microphone amplifier and the phase shift of the measurement system are canceled in this computation. This advantage enables us to use a relatively long probe-microphone without calibration in order to reduce the disturbance of the acoustic field of measurement space.

2.2 Experimental Setup

The specimens are mounted on a plane baffle. SPD's ($P(\mathbf{r})$ and $\phi(\mathbf{r})$) are measured frequency by frequency using a probe microphone installed on a computer controlled mechanical XY-stage. The details of this measurement system are described in [2]. The positioning accuracy of the probe microphone is important since spatial gradients of $P(\mathbf{r})$ and $\phi(\mathbf{r})$ are required to compute $\mathbf{v}(\mathbf{r})$. The XY-stage is driven by pulse motors with an absolute positioning accuracy being better than 10 μm.

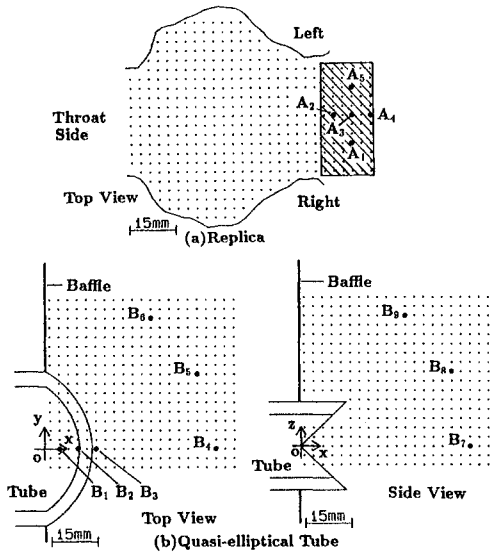

Fig.1 Measurement positions.

2.3 Specimens

Two specimens are used for experiment. One is a plaster replica of the lips and oral cavity. SPD's for this replica have already been measured and reported in [2]. These SPD's in the lip region are used to compute the acoustic impedance density. Fig.1(a) shows a measurement plane of the replica. This plane is located horizontally at the mid-height between upper and lower dental arches. Dots represent measurement positions of sound pressure and hatched area indicates the lip region. The other specimen is a quasi-elliptical uniform tube with its end cut in wedged-shape in order to imitate a protrusive lip shape. This tube was made by severing a plexiglass tube of an inner diameter of 50 mm into two pieces longitudinally and then gluing them together resulting in the sectional area of 5.8 cm^2. This specimen is mounted on the plane baffle with the deepest points of the wedged-shaped cut to be located just on the baffle surface. Fig.1(b) shows horizontal and vertical measurement planes for this specimen. The spacing between measurement positions is 3.0 mm.

3. EXPERIMENTAL RESULTS

3.1 Near Field of Lip Replica

Fig.2(a) shows the frequency characteristics of $Z_d(\mathbf{r})$ at measurement positions A_1,A_3, and A_5, and Fig.2(b) $Z_d(\mathbf{r})$ at positions A_2,A_3, and A_4 (see Fig.1(a) for these positions). Both real and imaginary parts of $Z_d(\mathbf{r})$ are normalized by characteristic impedance Z_0 (= ρc) of air. It is seen in Fig.2(a) that $Z_d(\mathbf{r})$ is quite symmetrical with respect to the midsagittal line with decreasing in gross as the position changes in lateral direction. It might be considered that these curves are radiation impedance density if each measurement position is regarded as a *boundary* at the lips. However, a small change in position in the lip region, especially in the anterior-posterior direction gives a large change in $Z_d(\mathbf{r})$, which implies that these positions are not suitable to set a *boundary condition* for numerical computation. A large variation of $Z_d(\mathbf{r})$ in the anterior-posterior direction may be understood if we assume forward and backward wave components at the lip region and define a hypothetical reflection coefficient $\mu(\mathbf{r}) = (Z_0 - Z_d(\mathbf{r}))/(Z_0 + Z_d(\mathbf{r}))$ from well known transmission line theory. Amplitude and phase characteristics of $\mu(\mathbf{r})$ are shown in Fig.3. An increase of linear phase lag is seen as the measurement position changes in the posterior direction while the magnitude is not greatly influenced by the position change. These characteristics indicate that the labial horn acts as an acoustic wave guide of a certain length, which confirms previous experimental results obtained from acoustic input-impedance measurement[6,7].

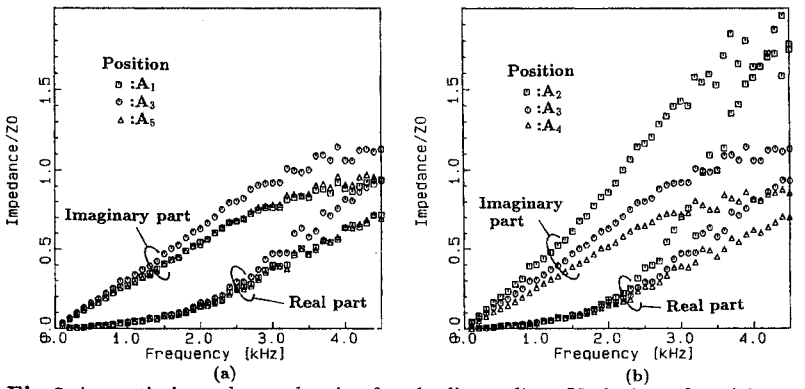

Fig.2 Acoustic impedance density for the lip replica. Variation of positions (a) in the transverse direction, and (b)in the anterior-posterior direction.

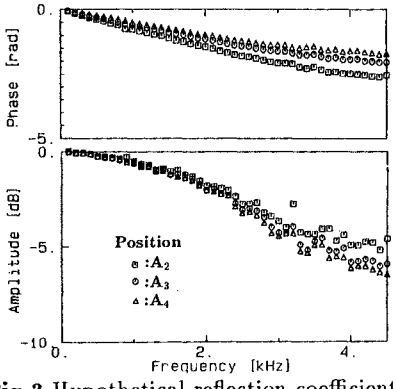

Fig.3 Hypothetical reflection coefficient characteristics corresponding to Fig.2(b).

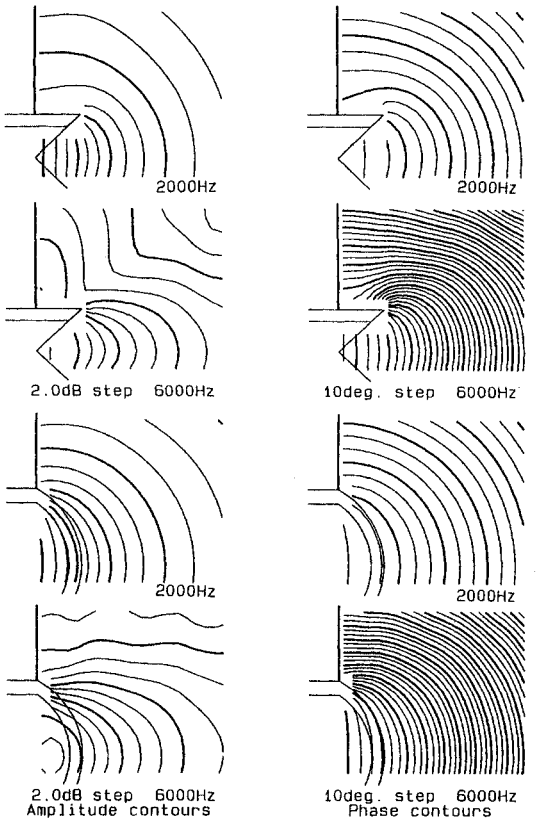

Fig.4 Amplitude (left panels) and phase (right panels) contours of sound pressure distribution.

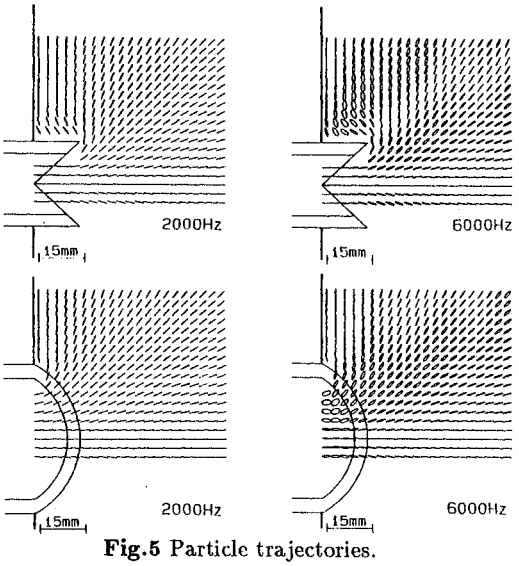

Fig.5 Particle trajectories.

3.2 Near Field of Wedged-Shaped Cut

The SPD's in the near field of the wedged-shaped cut at 2 and 6 kHz are shown in Fig.4. The contour intervals of amplitude and phase are 2.0 dB and 10 Deg., respectively. The particle trajectories for both frequencies are shown in Fig.5. The length of the major axis of each trajectory is set constant in order to emphasize the vibration pattern of medium. Medium particle motion follows almost straight lines at every points at 2 kHz while quite elliptical trajectories are seen at 6 kHz in the lateral portion of the radiating region. The aspect ratio of the major and minor axes of elliptical trajectory shows

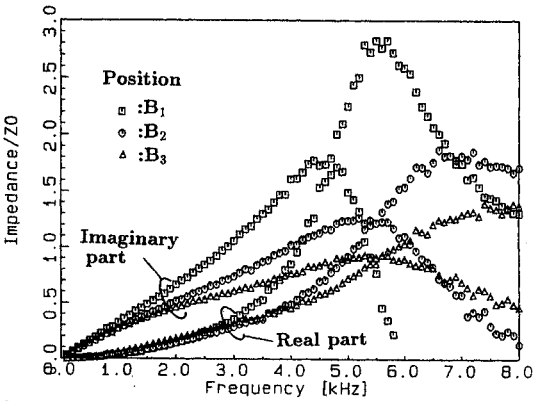

Fig.6 Variation of acoustic impedance density in anterior-posterior direction at the wedged-shaped cut.

the degree of one-dimensionality of the medium motion. Thus the map of particle trajectory may be used for defining the boundary surface for numerical computation, since one-dimensional motion is preferable on the boundary. In the vertical section, diffraction due to the sharp edges of our specimen is seen from the deformed pattern of amplitude contours and the phase circulation around these edges. Fig.6 shows frequency characteristics of $Z_d(\mathbf{r})$ at positions B_1,B_2, and B_3 in Fig.1(b). Again, we see the strong dependency of $Z_d(\mathbf{r})$ on the position in the radiating area, as for the replica. This is likely due to the effect of the upper and lower edges of this simplified lip horn. Fig.7 shows $Z_d(\mathbf{r})$'s at the different positions $B_4 \sim B_9$, located at a distance of 55.0±0.5mm from the origin o (see Fig.1(b)) on the baffle, the intersection point between the vertical and horizontal planes of symmetry for this tube. It should be recalled that $Z_d(\mathbf{r})$ is computed in the direction of the major axis of the elliptical particle trajectory at each frequency. It is clearly seen that the real part of $Z_d(\mathbf{r})$ approaches Z_0 with the ascent of frequency while the imaginary part approaches 0, and these characteristics are less direction sensitive. We also confirmed that the increase of the distance from the origin o lowers the frequency where the real and imaginary parts of $Z_d(\mathbf{r})$ intersect. These results suggest that a simple model of impedance density distribution can be used in the vicinity of the radiating region.

4. BOUNDARY CONDITION MODEL

It is of interest to know the spatial distributions of $Z_d(\mathbf{r})$ for simple radiation models: idealized elliptical piston set in an infinite baffle and a pulsating sphere of a certain radius. Although a wave equation for an elliptical waveguide can be solved using special functions[8], it is difficult to obtain an analytical formulation giving $Z_d(\mathbf{r})$ for the elliptical piston. However, we can approximately compute velocity potential $\Phi(\mathbf{r})$ as follows, by replacing the surface integral over the surface S of the elliptical piston by the summation of a number of small area elements ΔS_i.

$$\Phi(\mathbf{r}) = \frac{1}{2\pi}\int\int_S \frac{v_0}{r'}e^{-jkr'}dS \approx \frac{1}{2\pi}\sum_i \frac{v_0}{r'_i}e^{-jkr'_i}\Delta S_i \quad (5)$$

where v_0 is a given vibration velocity of the piston surface, k is the wave number, and i denotes the i-th area element, and r'_i a distance between ΔS_i and $\mathbf{r}$. Then we can obtain the complex sound pressure $p(\mathbf{r}) = j\omega\rho\Phi(\mathbf{r})$, and finally $Z_d(\mathbf{r})$ is computed in the same way as in the experiment. For this computation, the elliptical piston is specified as having an area of 5.8 cm^2 and an aspect ratio, *i.e.* the ratio of the length of the major axis to

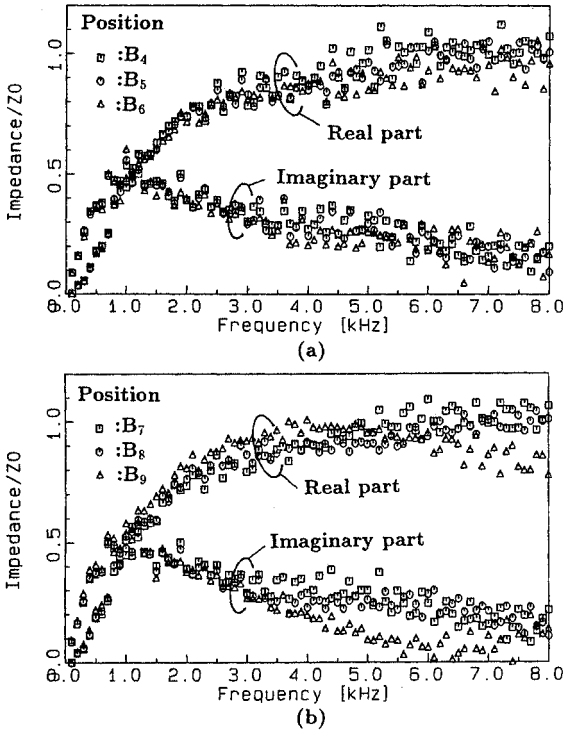

Fig.7 Variation of acoustic impedance density in angular direction with constant distance from the origin. (a)Horizontal plane. (b)Vertical plane.

that of minor axis, of 2.0, which is an approximation of the cross-sectional area and shape of the plexiglass specimen used in the experiment. The surface of the piston is divided into 15708 small square elements. Symbols in Fig.8 show $Z_d(\mathbf{r})$'s at two different positions on a plan containing the major axis of the elliptical piston. One is that on a central axis, a line normal to the center of the piston, at a distance of 54 mm from the piston center (represented by *circles* in Fig.8), and the other is at a position with the same distance but in an oblique direction of 52 degrees from the central axis (*squares*). At the latter position, the angle of the major axis of particle trajectory from the central axis, which indicates the dominant direction of medium vibration, is computed as about 49 degrees in all frequencies from 100 Hz to 8 kHz. The one-dimensionality of the medium motion can be examined by computing the aspect ratio of the particle trajectory. The aspect ratio decreases monotonically with the ascent of frequency, and is 130, 16.3 and 6.5 at 1, 4 and 8 kHz, respectively. It should be noted that, although the one-dimensionality of the medium motion at the latter position decreases with frequency, there is no significant difference in $Z_d(\mathbf{r})$'s for these two positions.

While $Z_d(\mathbf{r})$ computation based on eq.(5) requires relatively complicated procedures, $Z_d(\mathbf{r})$ on the surface of the pulsating sphere is obtained straightforward as,

$$Z_d(\mathbf{r}) = \frac{jk|\mathbf{r}|}{1+jk|\mathbf{r}|}\rho c. \qquad (6)$$

where $|\mathbf{r}|$ is the radius of the sphere. $Z_d(\mathbf{r})$, for $|\mathbf{r}| =$ 54mm, is shown in solid lines in Fig.8 as well, and is similar to the results of the elliptical piston model. These results suggest that, if the boundary surface for FEM computation is determined in the vicinity of the radiating region, it would be valid to assume that $Z_d(\mathbf{r})$ depends not on the direction, but on the distance from the center of the radiating region, and could be easily

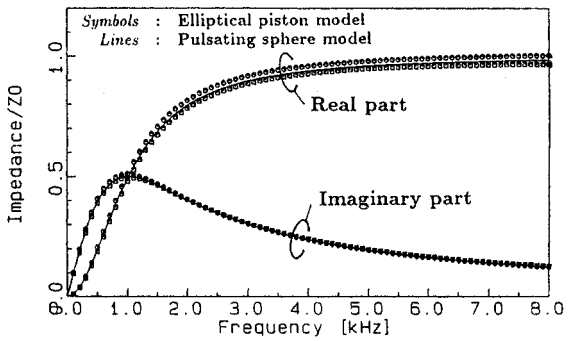

Fig.8 Acoustic impedance density for simple radiation models. Circles: 54mm from the piston center, squares: 54mm from the piston center in an oblique direction of 52 degrees, solid lines: pulsating sphere of 54mm radius.

obtained from eq.(6). The boundary surface should be normal to a radial line from the center of the radiating region in this case. Comparison between Fig.8 and Fig.7 confirms that, even though the radiating horn has a complex shape, there is a region, not too far away from the center of the radiating region (54 mm in this case), where the measured $Z_d(\mathbf{r})$ is similar to that of a simple pulsating sphere.

5. CONCLUDING REMARKS

The acoustic impedance density $Z_d(\mathbf{r})$ was determined from complex sound pressure distributions for two specimens. It was shown that the acoustic impedance density $Z_d(\mathbf{r})$ derived from a simplified radiation model, such as a pulsating sphere for instance, could be used as boundary condition for FEM computation. This could help reducing the number of finite elements of the radiating region.

ACKNOWLEDGEMENT

This work was supported by a Grant-in-Aid for International Scientific Research Program (05044072) from the Ministry of Education, Japan.

REFERENCES

[1] K.Motoki, N.Miki, and N.Nagai, "Measurement of sound wave characteristics in the vocal tract," Proc. ICSLP90, 433-436(1990).

[2] K.Motoki, N.Miki, and N.Nagai, "Measurement of sound-pressure distribution in replicas of the oral cavity," J. Acoust. Soc. Am., **92**, 2577-2585(1992).

[3] C.Lu, T.Nakai, and H.Suzuki, "Finite element simulation of sound transmission in the vocal tract," J. Acoust. Soc. Jpn.(E), **14**, 63-72(1993).

[4] H.Matsuzaki, T.Hirohku, N.Miki, and N.Nagai, "Three dimensional FEM analysis of sound tube with distributed non-uniform wall impedance," Proc. Autumn Meet. Acoust. Soc. Jpn., 3-6-7 (1993) (in Japanese).

[5] A.Ishida, N.Takahashi, T.Nakai, and H.Suzuki, "Simulation of acoustic tube model of vocal tract with 3-dimensional Finite Element Method," Proc. Autumn Meet. Acoust. Soc. Jpn., 3-P-30(1993) (in Japanese).

[6] K.Motoki, N.Miki and N.Nagai, "Measurement of radiation characteristics using replicas of the lips," J. Acoust. Soc. Jpn.(E), **9**,123-130(1988).

[7] P.Badin, K.Motoki, N.Miki, D.Ritterhaus, and M.T. Lallouache, "Some geometric and acoustic properties of the lip horn," J. Acoust. Soc. Jpn. (E), **15**,243-253(1994).

[8] A.Hasegawa, "Comparisons of sound propagation in rigid-walled and soft-walled elliptical waveguides," J. Acoust. Soc. Jpn., **32**, 703-709 (1976) (in Japanese).